Phase Relation of Harmonics in Nonlinear Focused Ultrasound *

Zhe-Fan Peng(彭哲凡)[1], Wei-Jun Lin(林伟军)[1**], Shi-Lei Liu(刘石磊)[2], Chang Su(苏畅)[1], Hai-Lan Zhang(张海澜)[1], Xiu-Ming Wang(王秀明)[1]

[1]*State Key Laboratory of Acoustics, Institute of Acoustics, Chinese Academy of Sciences, Beijing 100190*
[2]*Key Laboratory of Modern Acoustics, Department of Physics, Collaborative Innovation Center of Advanced Microstructure, Nanjing University, Nanjing 210093*

(Received 12 April 2016)

The phase relation of harmonics in high-intensity focused ultrasound is investigated numerically and experimentally. The nonlinear Westervelt equation is solved to model nonlinear focused sound field by using the finite difference time domain method. Experimental waveforms are measured by a robust needle hydrophone. Then the relative phase quantity is introduced and obtained by using the zero-phase filter. The results show that the nth harmonic relative phase quantity is approximately $(n-1)\pi/3$ at geometric center and increases along the axial direction. Moreover, the relative phase quantity decreases with the increase of source amplitude. This phase relation gives an explanation of some nonlinear phenomena such as the discrepancy of positive and negative pressure.

PACS: 43.25.+y, 43.80.+p DOI: 10.1088/0256-307X/33/8/084301

High intensity focused ultrasound (HIFU) is an evolving noninvasive therapy in recent years. The principle of HIFU is to raise the targeted tissue temperature to relatively high values to destroy the pathogenic tissue rapidly through ablation, while leaving the surrounding healthy tissue minimally affected.[1,2] In this process, some nonlinear phenomena such as the amplitude discrepancy and the peak position shift of the positive and negative pressure are observed.[3–5] In the ultrasound therapy, the positive pressure is associated with the thermal effect while the negative part determines the cavitation effect. Consequently, the amplitude discrepancy in the nonlinear sound field enhances the thermal effect with respect to the linear condition. Hamilton *et al.*[6] suggest that these nonlinear phenomena are related to the harmonic phase shifts introduced by diffraction. Thus there is a stimulus to study the phase relation of harmonics to give an explanation of these phenomena.

Some researchers have investigated phase information of harmonic components in nonlinear acoustic fields. Lucas *et al.*[7] derived the second harmonic solution of nonlinear focused model under the quasilinear approximation in integral form and introduced the relative phase quantity of the second harmonic. Saito *et al.*[8] used the same method and obtained the relative phase quantity 0.35π radians at the focus. However, the quasilinear method fails to calculate the energy transmitting of different harmonic components and absorption in the media. Therefore this method cannot describe the phase variation adequately. Other analytical and numerical methods were used to calculate the phase information as well.[9,10] These investigations utilized the paraxial approximation, thus they can only describe the acoustic field radiated by small aperture transducer. In addition, these researchers did not make much discussion about the phase relation between harmonics. In recent years, few research studies about phase information have been reported. Further research into phase analysis of different harmonic components is needed to have a better understanding of the nonlinear phenomena in nonlinear focused ultrasound.

In this Letter, a nonlinear focusing model based on the Westervelt equation and an experiment are performed to investigate the phase relation between harmonic components and its influence on positive and negative pressures. The concept of relative phase quantity which represents the phase relation between harmonics is also introduced. It is worth noting that the results are only valid before the formation of a shock wave. Moreover, relative phase quantity in the soft tissue model is considered.

A nonlinear acoustic focused model is shown in Fig. 1. The nonlinear acoustic wave field in inhomogeneous thermoviscous media can be described by the modified Westervelt equation introduced by Hamilton *et al.*[11]

$$\nabla^2 p - \frac{1}{\rho_0}\nabla\rho_0\cdot\nabla p - \frac{1}{c_0^2}\frac{\partial^2 p}{\partial t^2} + \frac{\delta}{c_0^4}\frac{\partial^3 p}{\partial t^3} + \frac{\beta}{\rho_0 c_0^4}\frac{\partial^2 p^2}{\partial t^2} = 0, \quad (1)$$

where p is the sound pressure, c_0 is the speed of sound, ρ_0 is the density, $\beta = 1 + B/2A$ is the coefficient of nonlinearity with B/A being the parameter of nonlinearity of the fluid, and $\delta = 2\alpha c_0^3/\omega^2$ is the sound diffusivity with α being the attenuation coefficient and ω being the angular frequency. Due to the symme-

*Supported by the National Natural Science Foundation of China under Grant Nos 41274134 and 81527901, and the '12th Five-Year Plan' Period for Informatization Project in Supercomputing Key Demonstration of Chinese Academy of Sciences under Grant No XXH12503-02-02-2(07).

**Corresponding author. Email: linwj@mail.ioa.ac.cn

© 2016 Chinese Physical Society and IOP Publishing Ltd

try of the model, the simulation can be performed in cylindrical coordinate. The Laplace operator can be described as $\nabla^2 p = \partial^2 p/\partial r^2 + 1/r \cdot \partial p/\partial r + \partial^2 p/\partial z^2$. Mur's absorbing boundary condition is used to prevent artificial reflection.[12] The source condition of a uniform focused circular transducer can be expressed as

$$p_{\rm src} = p_0 \sin \omega t, \quad r \le a. \tag{2}$$

The geometric parameters of the focused transducer model are radius $a = 3.0\,$cm, and focal length $d = 7.5\,$cm. The half-aperture angle γ is 23.6°. The transducer is driven by a 1 MHz continuous wave. The pressure on the transducer surface is 0.2 MPa. The parameters of the medium (water) used in the simulation model are[13] $\rho_0 = 1000\,{\rm kg/m^3}$, $c_0 = 1500\,{\rm m/s}$, $\beta = 3.5$ and $\alpha = 0.02\,{\rm Np/m}$. The numerical implementation of Eq. (1) is performed by using the finite difference time domain (FDTD) method. The second-order differential scheme in time domain and fourth-order in space domain are conducted.[14] The time step is set to $\Delta t = 5 \times 10^{-9}\,$s and spatial step is $\Delta z = \Delta r = 4 \times 10^{-5}\,$m, which is approximately 1/40 of a wavelength to describe high harmonics accurately. The discretization steps satisfy the stability condition.

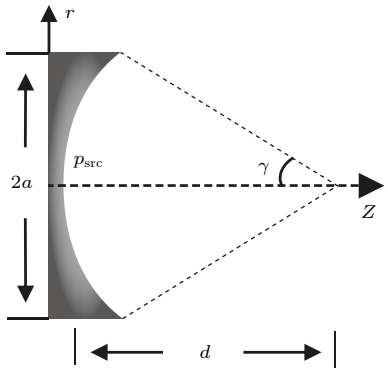

Fig. 1. Illustration of the nonlinear acoustic focused model.

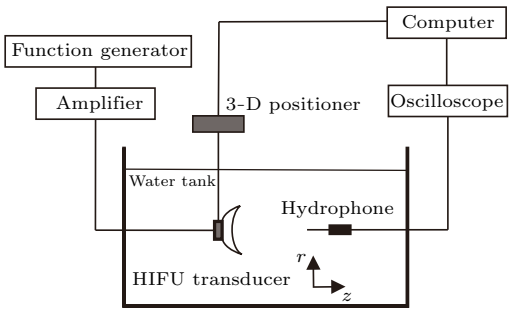

Fig. 2. Experimental arrangement for the measurement of nonlinear waveforms.

A diagram of the experimental arrangement to measure nonlinear waveform is shown in Fig. 2. A 1.12-MHz single element HIFU transducer with the radius of 5.0 cm and the focal length of 10.3 cm is used in the experiment. The transducer is attached to a three-dimensional positioning system. A pulse mode with a 25-cycle sin-wave burst signal is excited by a function generator (Agilent33250A, CA, USA) and amplified by an amplifier (ENI2200L, NY, USA). Waveforms are recorded by a robust needle hydrophone (ONDA HNA0100, CA, USA), which can measure the pressure up to 20 MPa. The waveforms from the hydrophone are averaged for eight times by the oscilloscope (Agilent 54830B, CA, USA) to improve the signal-to-noise ratio. A custom LABVIEW program is used to control the 3-dimensional positioning system and to save the waveforms. The water is purified and degassed to limit cavitation.

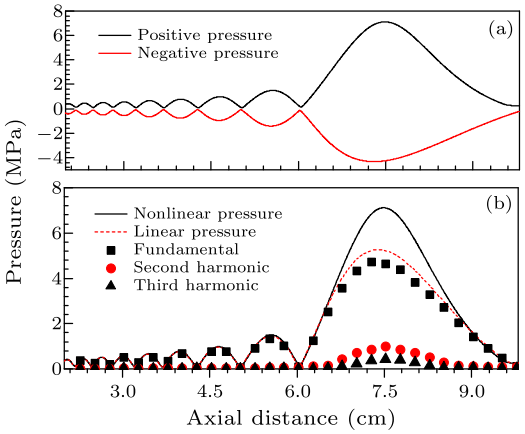

Fig. 3. Amplitude distribution simulated by the Westervelt equation. (a) Amplitude distributions of positive and negative pressures along the z-axis. (b) Amplitude distributions of harmonic components and linear pressure along the z-axis.

The amplitude distributions of positive and negative pressures along the z-axis from simulation are shown in Fig. 3(a). The simulated maximum positive pressure is 7.1 MPa while the minimum negative pressure is −4.3 MPa. The nonlinear positive focusing gain is 35.5 while the negative focusing gain is 21.5. The positive peak appears at 74.8 mm from the transducer while the negative peak appears at 72.9 mm. The positive pressure is much larger than that of the negative pressure, and the positive peak position is also closer to the geometric center of the transducer. Figure 3(b) shows the distributions of nonlinear positive pressure, linear pressure (set the nonlinearity and absorption terms to zero), fundamental, second and third harmonic components along the z-axis. From Fig. 3(b) it is shown that the positive pressure is larger than the linear pressure at the focus. The harmonic components can only be observed obviously around the focal zone. The amplitude of the fundamental component is lower than the linear pressure amplitude, which is due to the fact that the energy of the fundamental component transmits to the harmonic components.

Fundamental and harmonic waveforms can be extracted from the nonlinear waveform by using the zero-phase band-pass filter. Figure 4(a) shows the waveform at the focus and the superposition waveform of the first four harmonics obtained by digital signal

processing. These two waveforms agree well with each other due to the fact that the amplitudes of harmonic order larger than four are small in this case, indicating the validity of using the zero-phase filter. The positive part is sharpened and the negative part is extended. The waveform at the any axial position can be written as

$$p = \sum_{n=1}^{\infty} P_n \sin[n(\omega t - kz) - \theta_n], \tag{3}$$

where P_n and θ_n are the amplitude and the phase of the nth harmonic wave respectively, n means the order of harmonics, and k is the wave number. The phase of different harmonics cannot be compared directly, thus a relative phase quantity that describes relative phase of different harmonics and relates directly to the shape of the waveform is introduced,[7]

$$\theta_{n1} = \theta_n - n\theta_1. \tag{4}$$

Figure 4(b) shows the waveforms of the fundamental and second harmonic components. It should be noted that the second harmonic wave is delayed in time with respect to the fundamental wave. Thus the relative phase quantity can also be obtained from the extracted waveforms of fundamental and harmonic components. The obtained relative phase quantity can be expressed as

$$\theta_{n1} = \theta_n - n\theta_1 = 2\pi \frac{\Delta t_n}{T_n}, \tag{5}$$

where T_n is the cycle of the nth harmonic wave, and Δt_n is the time delay of the nth harmonic with respect to fundamental component, i.e., the interval of arriving time between the zero phase points of harmonic and fundamental wave as marked in Fig. 4(b) (Δt_2 as an example).

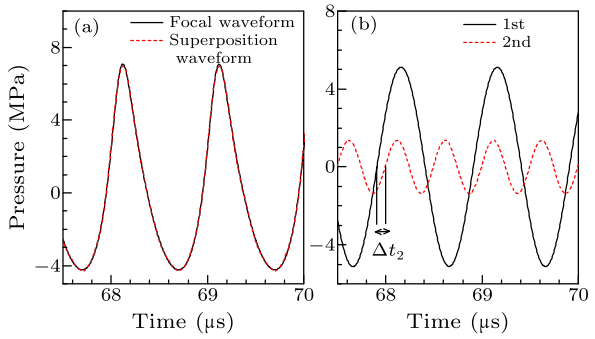

Fig. 4. (a) Waveform at the focus and superposition waveform of first four order harmonics, and (b) waveforms of two harmonic components obtained from the zero-phase band-pass filter, with the simulation result.

Under the linear condition, the focused acoustic field can be evaluated by the O'Neil integral formula, which can describe the acoustic field generated by a large aperture transducer. The pressure at the focus can be expressed as[15]

$$p = ip_0 k \frac{a^2 sec^2\alpha}{2d} e^{i(\omega t - kd)} = p_0 k \frac{a^2 sec^2\alpha}{2d} e^{i(\omega t - kd + \frac{\pi}{2})}, \tag{6}$$

where the nth harmonic frequency is n times the fundamental frequency. According to Eqs. (3), (4) and (6), the relative phase quantity in the linear condition can be obtained, i.e., $\theta_{n1} = \theta_n - n\theta_1 = -\pi/2 - n(-\pi/2) = (n-1)\pi/2$. This means that the relative phase quantity is $(n-1)\pi/2$ when only diffraction is considered.

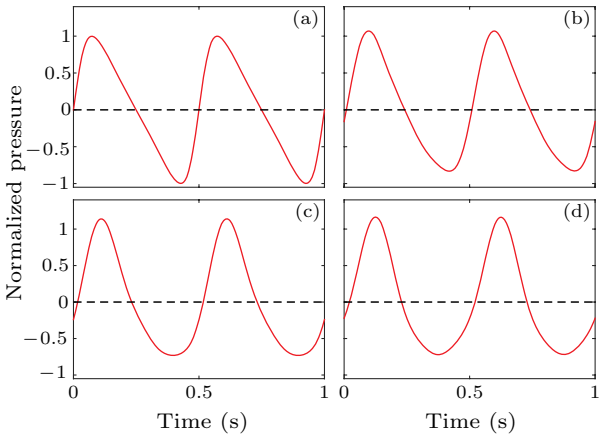

Fig. 5. Hypothetical waveforms for relative phase quantity (a) $\theta_{n1} = 0$, (b) $\theta_{n1} = (n-1)\pi/6$, (c) $\theta_{n1} = (n-1)\pi/3$, and (d) $\theta_{n1} = (n-1)\pi/2$.

Figure 5 shows the hypothetical normalized waveforms when the second harmonic and third harmonic amplitudes are 1/4, 1/16 of the fundamental amplitude respectively for relative phase quantities 0, $(n-1)\pi/6$, $(n-1)\pi/3$ and $(n-1)\pi/2$. In Fig. 5(a), the amplitudes of positive and negative parts are equal to 1. According to the Bessel–Fubini solution

$$p = p_0 \sum_n \frac{2J_n(nz/z_k)}{nz/z_k} \sin[n(\omega t - kz)], \tag{7}$$

where z_k is the shock formation distance, in nonlinear one-dimensional waves like plane waves, and no diffraction occurs, we obtain $\theta_n = 0$ and $\theta_{n1} = 0$ in any position. Although harmonic components are generated, the amplitudes of positive and negative pressures are still the same, which are similar to the situation in Fig. 5(a). In Fig. 5(d), the relative phase quantity is $(n-1)\pi/2$, which is linear focusing situation described in the previous paragraph. If sinusoidal waves of frequencies f, $2f$ and $3f$ are emitted simultaneously from a focusing transducer, the pressure profile at the focus will be similar to Fig. 5(d). As shown in Fig. 5, the discrepancy between positive and negative amplitudes increases with θ_{n1}. The largest discrepancy is observed in Fig. 5(d).

In the nonlinear focused acoustic field, the harmonics are generated and accumulated during the propagation. The diffraction introduces phase shifts between the nonlinearly generated harmonics. Hence, not only diffraction but also nonlinearity should be considered. Figure 6 shows the simulation result of second, third and fourth harmonic phase quantity distributions along the z-axis near the focus. The vertical

line is the position of the geometric center. Relative phase quantity is approximately $(n-1)\phi$ and increases along the axis. Here ϕ is about $\pi/3$ at the geometric center. This corresponds to the situation in Fig. 5(c). The region outside the focal zone is not discussed due to the fact that the amplitudes of harmonic components are low.

In pre-shock nonlinear propagation, generally the fundamental amplitude is larger than harmonic amplitude. Therefore we can use the fundamental pressure as reference. Then, the amplitudes of positive and negative pressure distributions on the z-axis can be written as

$$p_+(z) = P_1(z) + \sum_n P_n(z) \sin\left[\frac{n\pi}{2} - \theta_{n1}(z)\right],$$
$$p_-(z) = -P_1(z) + \sum_n P_n(z) \sin\left[-\frac{n\pi}{2} - \theta_{n1}(z)\right], \quad (8)$$

where P_1 and P_n are the amplitudes of fundamental and harmonic components, and $+\pi/2$ and $-\pi/2$ on the right side of the equation denote the phase of peak and trough, respectively. When θ_{n1} is equal to $(n-1)\pi/3$ as in the simulation result, the harmonic components P_2 and P_3 enlarge the value of p_+. On the contrary, P_2 diminishes the value of p_-. That is the reason why positive pressure is larger than negative pressure around the focus in nonlinear focused ultrasound. The peak positive is at a position closer to the geometric center where θ_{n1} is relatively high, while the peak position of p_- is closer to the transducer where θ_{n1} is relatively low. This explains the phenomena of the different peak positive and negative positions.

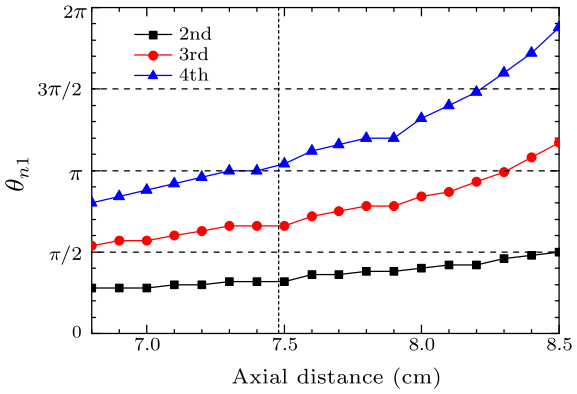

Fig. 6. Second-to-fourth order relative phase quantity distributions along the z-axis at focal zone simulated by Westervelt equation.

Higher exciting pressure leads to stronger nonlinear effects. Figure 7 shows the relative phase quantities at the geometric center for the exciting pressure $p_0 = 0.1$, 0.2, 0.3, 0.4 and 0.5 MPa. For low amplitude $p_0 = 0.1$ MPa, the phase quantity is $(n-1)\pi/3$. With the increase of nonlinearity, the phase quantity gradually deceases. According to Eq. (8), with more harmonic generated in stronger nonlinear focusing, the discrepancy between positive and negative is larger, and peak positive and negative position changes due to the complex combined effects of P_1, P_n and θ_{n1}. The distribution of these parameters along the z-axis can be found in Figs. 3(b) and 6. The changes of positive and negative peak positions with the exciting pressure can be found in Refs. [5,16].

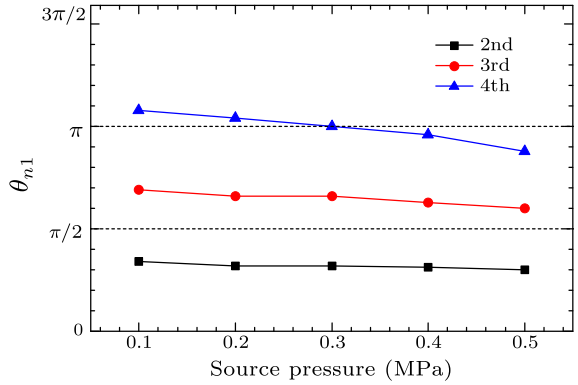

Fig. 7. Relative phase quantities of second-to-fourth harmonics with respect to fundamental component for different source pressures, with the simulation result.

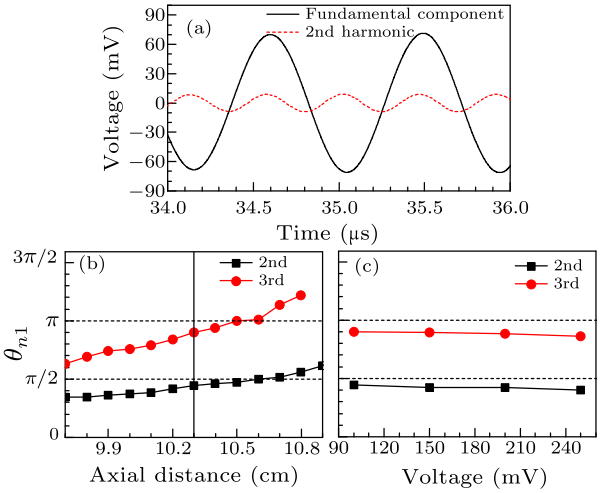

Fig. 8. Experimental result: (a) fundamental and second harmonic waveforms measured with robust needle hydrophone for input voltage 100 mV, (b) the experimental relative phase quantity along the z-axis at the focal zone obtained by the zero-phase filter, (c) relative phase quantities of 2nd and 3rd harmonics with respect to fundamental component.

An experiment is conducted to verify the simulation result. Nonlinear waveforms are measured with a robust needle hydrophone. The harmonic waveforms and relative phase quantities can be obtained by the zero-phase filter. Figure 8(a) shows the waveforms of fundamental and second harmonic components. Different arriving time of zero point is observed between fundamental and second harmonic waves which is similar to the simulation results in Fig. 4(b). Figure 8(b) shows the experimental results of relative phase quantities along the z-axis near the focus with an input voltage of 100 mV. Although the transducer used in the experiment has a different size from the simula-

tion model, the distribution pattern is similar, e.g., the relative phase quantity $(n-1)\phi$ is increasing along the z-axis. Here ϕ is larger than $\pi/3$ at the geometric center due to size difference of the transducer, but is still below $\pi/2$ as the simulation results. Figure 8(c) shows the measured θ_{n1} for different exciting voltages. Similar phase quantity variation tendency is observed at the geometric center: as the exciting power increases, the phase quantity slightly deceases. The relative phase quantity of higher exciting voltage is not presented due to the fact that the measuring amplitude upper limit of hydrophone is 20 MPa.

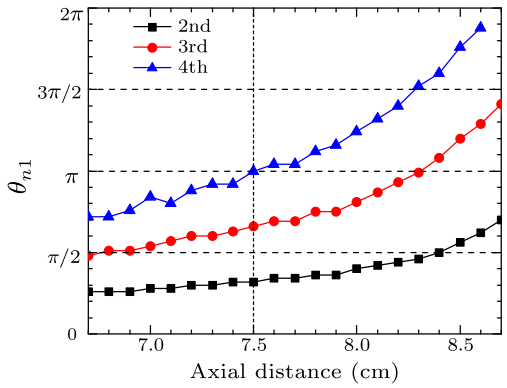

Fig. 9. Second-to-fourth order relative phase quantity distributions along the z-axis at the focal zone in layer tissue simulated with the Westervelt equation.

One simulation model of nonlinear focusing in human tissue is also investigated. A layer of soft tissue (muscle) with a thickness of 6 cm is inserted into the simulation model. The distance between the layer and the center of the transducer is 4 cm. The muscle's parameters are[17] $\rho_0 = 1130\,\mathrm{kg/m^3}$, $c_0 = 1566\,\mathrm{m/s}$, $\beta = 4.9$, $\alpha = 8.1\,\mathrm{Np/m}$. Other parameters are the same as the previous simulation model except for the exciting pressure $p_0 = 0.3\,\mathrm{MPa}$. Figure 9 shows the second, third and fourth order phase quantity distributions along the z-axis near the focus. Even though the absorption of tissue is much higher than water and the diffraction pattern may be affected by the water–tissue interface, the relative phase quantity follows the same tendency as in water, indicating that layered tissue has negligible effects on relative phase quantity due to the limit difference of acoustic impedance.

In conclusion, the nonlinear Westervelt equation has been solved and the corresponding experiment has also been carried out to investigate the phase relation in the high intensity focused ultrasound. The relative phase quantity has been obtained using a zero-phase filter. Experimental and simulation results show that the relative phase quantity is approximately $(n-1)\pi/3$ at the focal zone. As a consequence, the interference among harmonic components enhances the peak and damps the trough in the full waveform. This explains why the amplitude of positive pressure is much larger than that of negative pressure. In addition, strong nonlinear effect decreases the phase quantity slightly at the focus and the soft tissue boundary has negligible diffraction effects on phase quantity. The phase relation reported in this work is a universal phenomenon in nonlinear focused ultrasound.

References

[1] ter Haar G and Coussios C 2007 *Int. J. Hyperthermia* **23** 89
[2] Wu F, Wang Z B, Chen W Z, Zou J Z, Bai J, Zhu H, Li K Q, Xie F L, Jin C B, Su H B and Gao G W 2004 *Ultrasound Med. Biol.* **30** 245
[3] Chen T, Qiu Y Y, Fan T B and Zhang D 2013 *Chin. Phys. Lett.* **30** 074302
[4] Canny M S, Bailey M R, Crum L A, Khokhlova V A and Sapozhnikov O A 2008 *J. Acoust. Soc. Am.* **124** 2406
[5] Camarena F, Adrián-Martínez S, Jiménez N and Sánchez-Morcillo V 2013 *J. Acoust. Soc. Am.* **134** 1463
[6] Hamilton M F, Khokhlova V A and Rudenko O V 1997 *J. Acoust. Soc. Am.* **101** 1298
[7] Lucas B G and Muir T G 1983 *J. Acoust. Soc. Am.* **74** 1522
[8] Saito S, Kim B C and Muir T G 1987 *J. Acoust. Soc. Am.* **82** 621
[9] Ding D, Shui Y, Lin J and Zhang D 1996 *J. Acoust. Soc. Am.* **100** 727
[10] Hart T S and Hamilton M F 1988 *J. Acoust. Soc. Am.* **84** 1488
[11] Hamilton M F and Blackstock D T 1998 *Nonlinear Acoust.* (San Diego: Academic Press) Chap **3** p 41
[12] Mur G 1981 *IEEE Trans. Electromagn. Compat.* EMC-23 **377**
[13] Fan T B, Liu Z B, Zhang Z, Zhang D and Gong X F 2009 *Chin. Phys. Lett.* **26** 084302
[14] Hallaj I M and Cleveland R O 1999 *J. Acoust. Soc. Am.* **105** L7
[15] O'neil H T 1949 *J. Acoust. Soc. Am.* **21** 516
[16] Makov Y N, Sánchez-Morcillo V J, Camarena F and Espinosa V 2008 *Ultrasonics* **48** 678
[17] Goss S A, Johnston R L and Dunn F 1978 *J. Acoust. Soc. Am.* **64** 423